Measurement of the 2_1^+ level lifetime in ^{120}Sn by the Doppler shift attenuation method: Evidence of enhanced collectivity

A. Kundu,[1,2,*] S. Santra,[1,2] A. Pal,[1,2] D. Chattopadhyay,[1,2] R. Raut,[3] R. Palit,[4] Md. S. R. Laskar,[4] F. S. Babra,[4] C. S. Palshetkar,[4] B. K. Nayak,[1,2] and S. Kailas[1,5]

[1]*Nuclear Physics Division, Bhabha Atomic Research Centre, Mumbai 400085, India*
[2]*Homi Bhabha National Institute, Anushakti Nagar, Mumbai 400094, India*
[3]*UGC-DAE Consortium for Scientific Research, Kolkata Centre, Kolkata 700098, India*
[4]*Department of Nuclear and Atomic Physics, Tata Institute of Fundamental Research, Mumbai 400005, India*
[5]*Manipal Center for Natural Sciences, Manipal Academy of Higher Education, Manipal 576104, India*

(Received 18 July 2019; published 30 September 2019)

Background: There has been a considerable interest focused on the study of enhancement or suppression in collectivity of the excited 2_1^+ states in stable Sn isotopes. Independent measurements of Coulomb excitation cross sections and 2_1^+ level lifetimes report discrepant transition probabilities. Existing estimates for 2_1^+ lifetime indicate reduced collectivity.

Purpose: A reexamination of lifetime of the 2_1^+ state in the most abundant ^{120}Sn isotope is thus warranted. The same has been carried out in the present work and the result has been used to determine the transition probability as an indicative of the underlying collectivity.

Methods: Low-lying levels in the vibrational ^{120}Sn nucleus have been excited by inelastic scattering with ^{32}S beam at $E_{\rm lab} = 120$ MeV. Level lifetime measurements have been carried out using the Doppler shift attenuation method, wherein the Doppler affected γ-ray peaks have been analyzed using updated methodologies.

Results: From the measured lifetime of the 2_1^+ state ($E_x = 1171$ keV) in ^{120}Sn, $\tau_{2_1^+} = 0.863^{+0.029}_{-0.036}$ ps, a value of $B(E2; 0^+_{\rm g.s.} \rightarrow 2_1^+) = 0.215^{-0.007}_{+0.009}$ is deduced. An estimate of the 4_1^+ (feeder) level lifetime, $\tau_{4_1^+} = 1.77^{+0.084}_{-0.089}$ ps, is also reported from lineshape analysis of γ rays in cascade.

Conclusions: An enhancement in collectivity for the 2_1^+ state is confirmed, following an improved determination of the level lifetime, with reduced uncertainties. The excited 2_1^+ state is also found to have a nonvanishing moment of inertia, suggesting anharmonic nature of quadrupole vibrations.

DOI: 10.1103/PhysRevC.100.034327

I. INTRODUCTION

The determination of lifetimes of excited states is one of the principal pursuits in nuclear structure measurements. The corresponding transition probabilities reveal dynamic deformations of the nuclear density and are the most direct and unambiguous test of the collective nature of the excitation modes. For transitions of multipolarity λ in nuclei, the electric transition probabilities, $B(E\lambda)$, are often measured via, e.g., Coulomb-excitation and light- or heavy-ion-scattering experiments. In a complementary approach, the $B(E\lambda)$ values can also be determined if the spin and parity of the states involved and the γ-decay branching ratio as well as the mean lifetime, τ, of the excited state are known.

There exists a significant correlation between the excitation spectra of nuclei obtained by electromagnetic decay and by nuclear scattering. This correlation is qualitatively observed when the low-lying 2_1^+ levels of doubly even spherical nuclei are studied; matrix elements for nuclear excitation in a direct interaction model are closely analogous to those for electric multipole radiation between the same two states [1]. In this context, the 2_1^+ state in the stable even-mass $^{112-124}$Sn isotopes has been extensively probed by means of Coulomb excitation [2–4], nuclear resonance fluorescence [5], and inelastic scattering of electron [6], proton [7], α [8], and heavy ions [9–11]. The transition probabilities, $B(E2; 0^+_{\rm g.s.} \rightarrow 2_1^+)$, often measured with smaller uncertainties, have been consolidated from several independent measurements into the adopted values by Raman *et al.* [12]. These values are enhanced over the Weisskopf single-particle estimates [13]. Existing theoretical estimates for excitations in $^{102-130}$Sn based on single j-shell exact seniority model [14], as well as large-scale shell-model calculations involving proton-core excitations [15] also suggest highly collective quadrupole transitions in the Sn isotopes, with a symmetric decrease in $B(E2)$ as the neutron number varies from the midshell ^{116}Sn nucleus on either side, following a parabolic behavior. This trend has been verified for the isotopes with mass $A > 116$ by $B(E2)$ measurements extending up to the unstable and neutron-rich $^{126-130}$Sn isotopes [16]. However, for $A < 116$, the $B(E2)$ values are found to increase first from ^{116}Sn to ^{112}Sn and stay nearly similar up to ^{106}Sn within experimental uncertainties, thereafter decreasing toward the

*ananyak.delhi@gmail.com

neutron-deficient ^{104}Sn [17–19]. The relativistic quasiparticle random-phase approximation (RQRPA) calculations for $^{100-136}$Sn [20] have been fairly successful in justifying the observed trend of the $B(E2)$ values for both the neutron-deficient as well as neutron-rich unstable isotopes, explaining the sudden increase at the $N = 82$ shell closure [16,21] as well as predicting a similar rise for the $N = 50$ shell closure. However, the RQRPA results are suppressed by up to ≈30% for the stable $^{112-124}$Sn isotopes compared to the adopted values. In the light of such discrepancies, unambiguous quantitative assessments of collective properties for the 2_1^+ level in the stable Sn isotopes, with better understood structures, could act as a reference for improved experimental and theoretical studies of the unstable isotopes near shell closure, that are expected to be of similar complexity.

Lately, a series of Coulomb excitation experiments on $^{112-124}$Sn, based on either direct estimation of $\tau_{2_1^+}$ [22,23], or direct measurement of $B(E2; 0^+_{\rm g.s.} \to 2^+_1)$ [24,25], have been reported with discrepant results. The $B(E2)$ values deduced from the level lifetimes reported by Jungclaus *et al.* [22] are considerably lower than the adopted values across the Sn isotopic chain, showing a departure from collectivity and with a shallow minimum at ^{116}Sn. These results have been much disputed later by Allmond *et al.* [25] and Kumar *et al.* [24]. Though the overall mass dependence of the $B(E2)$ values is similar in both these measurements, they report markedly different absolute values for the neutron-rich ^{120,122,124}Sn isotopes. The $B(E2)$ results of Kumar *et al.* [24] are apparently prone to normalization uncertainties as these quantities have been estimated relative to the $B(E2)$ value of the excited ^{58}Ni projectile used in this measurement, chosen to be equal to 0.065 e^2b^2, which is less than both the adopted value [12] as well as the average value from a recent compilation [26] of results of Coulomb excitation and electron-scattering measurements on ^{58}Ni. On the other hand, Allmond *et al.* [25] report a robust measurement of the $B(E2)$ values, along with the static electric quadrupole moments $Q_S(2_1^+)$ and magnetic dipole moments $g(2_1^+)$ for all the stable Sn isotopes to a high degree of precision in an inverse kinematics experiment. The $B(E2)$ results are in good agreement with the adopted values and predict an overall enhancement of collectivity.

There have been theoretical studies directed toward explaining the trend of low $B(E2)$ values, with a shallow minimum at ^{116}Sn, from the lifetime results reported by Jungclaus *et al.*, (i) employing two sets of effective charges across the Sn isotopic chain (for $A > 116$ and $A < 116$) for a shell-model Hamiltonian with monopole and quadrupole pairing, and quadrupole-quadrupole interaction between valence neutrons [27], and (ii) a schematic two-level, generalized seniority scheme concerned with the order of filling of the j orbits in the Sn isotopes [14]. However, to reproduce the aforementioned trend, these calculations predict $B(E2)$ values further smaller by ≈15–25%, particularly for the $^{114-120}$Sn isotopes. It may be mentioned that the lifetime analysis for ^{118,120,124}Sn by Jungclaus *et al.* employed a natural Sn target covered by a front layer of natural Pd, with γ rays detected in coincidence with ^{58}Ni projectiles backscattered from both Sn and Pd foils. Since the 2_1^+ excitation energies in the neighboring Sn isotopes are closely spaced, a demerit of this choice of target is an apparent overlap between the Doppler broadened high-energy tail of the lineshapes, particularly as seen for ^{120,122,124}Sn in Refs. [22,23]. Additionally, there could be contaminant γ energies from the Pd layer buried under the lineshapes from the Sn nuclei, e.g., the decay of long-lived levels in ^{106,108,110}Pd with γ energies in the range of 1180–1195 keV. This may amount to an erroneous estimation of lifetimes in this analysis. The lifetime for ^{120}Sn, $\tau_{2_1^+} \approx 1$ ps, is, however, found to be consistent with another measurement by Sie *et al.* [28] involving γ rays in coincidence with backscattered ^{35}Cl projectiles. As reported in Ref. [28], comparison of this lifetime with values inferred from absolute Coulomb excitation cross sections indicated a discrepancy, with this value being longer. An older measurement of $\tau_{2_1^+} =$ 1.26 ps for ^{120}Sn by nuclear γ-ray resonance absorption method [29] also puts the $B(E2)$ value in the region of much lower collectivity. This is in contrast to a complementary measurement [5] of angular distribution of photon-scattering cross section that reports a very high $B(E2)$ for ^{120}Sn. Recent heavy-ion-scattering measurements on the stable Sn isotopes with probes ^{7}Li [9] and ^{12}C [11] also report enhanced $B(E2)$ values, consistent with the results of Allmond *et al.* [25].

In order to address the large disagreements across different experiments, particularly for the most abundant ^{120}Sn isotope, a new measurement using updated techniques is warranted. The exercise is expected to facilitate concluding on the lifetime of the 2_1^+ state and, thus, the $B(E2, 0^+_{\rm g.s.} \to 2^+_1)$ value determined therefrom. The present work reports such a measurement of the 2_1^+ lifetime using the Doppler shift attenuation method (DSAM). This has been the technique of choice in the subpicosecond regime and is based on the analysis of Doppler affected γ-ray transition peaks emitted by nuclei produced in a reaction that deexcites in-flight while traversing through the target and/or the backing medium. The present work is dedicated to the measurement of level lifetime of the 2_1^+ state in ^{120}Sn ($E_x = 1171$ keV) that is populated by means of inelastic excitation predominantly under the effect of Coulomb interaction with a heavy-ion beam. The Doppler shape of the 1171-keV transition, following the deexcitation of the 2_1^+ state, has been analyzed as elaborated on in the subsequent text.

The paper is organized as follows. The experimental setup is described in Sec. II. The analysis procedure that explains the experimental spectra is described in Sec. III. The results and their importance are discussed in Sec. IV, and summarized in Sec. V.

II. MEASUREMENT

The low-lying excited states of ^{120}Sn nucleus have been populated using the ^{120}Sn(^{32}S, ^{32}S$'$)^{120}Sn* reaction at $E_{\rm lab} =$ 120 MeV. The ^{32}S beam was provided by the BARC-TIFR Pelletron LINAC Facility, Mumbai. A beam energy below the Coulomb barrier ($V_B \approx 123$ MeV) was chosen on the basis of coupled-reaction-channels (CRC) calculations (i) to minimize the contribution of the nuclear field in the excitation process, (ii) to have substantial inelastic-scattering cross section for the excitation of the 2_1^+ state in ^{120}Sn, (iii) to suppress the excitation of higher-energy states (such as higher multipolarities and/or multiphonon excitations) that could feed the nuclear level of our interest, and (iv) to minimize contamination from other reaction channels such as transfer of nucleon(s) and fusion ($\sigma_F < 1$ mb). The target comprised an enriched ^{120}Sn foil of thickness ≈6.4 mg/cm^2, with a ^{197}Au backing of thickness ≈6.2 mg/cm^2. The excitation is governed by well-defined two-body kinematics and energetics and predominantly mediated by the Coulomb interaction between the collision partners. Emitted γ rays from the recoiling ^{120}Sn nuclei have been detected using a segment of the Indian National Gamma Array (INGA) [30], then consisting of 11 Compton-suppressed segmented clover HPGe detectors, mounted at a distance of 25 cm from the target center. The clovers were distributed in the backward hemisphere with respect to the beam direction at $\theta = 90^\circ$ (three at $\phi = 60^\circ, 120^\circ, 300^\circ$), $\theta = 115^\circ$ (two at $\phi = 90^\circ, 330^\circ$), $\theta = 140^\circ$ (three at $\phi = 0^\circ, 120^\circ, 240^\circ$), and $\theta = 157^\circ$ (three at $\phi = 60^\circ, 180^\circ, 300^\circ$). Time-stamped list mode spectroscopic data have been acquired using a digitizer-based data acquisition system. The acquired decay events are sorted into spectra and E_γ-E_γ matrices using the MARCOS [31] code. The matrices were both symmetric as well as angle-dependent asymmetric for lifetime analysis. The latter had the 90° detectors on the x axis, with detectors at one of the other angles (157°, 140°, 115°) on the y axis. The detectors are calibrated in energy and efficiency using standardized ^{133}Ba-^{152}Eu source. A resolution of ≈2.6 keV has been obtained at an energy of 1408 keV.

In the singles spectra as shown in Fig. 1, a distinct Doppler broadened shape is observed for the $E2$ transition peak at 1171 keV, corresponding to the deexcitation of the 2_1^+ level in ^{120}Sn. The analysis of Doppler shapes following γ-ray measurements in singles mode, where the angular distribution of the recoiling ions is given by inelastic-scattering theory, bears the advantage of improved counting statistics when compared to a coincidence measurement for $E_{\rm lab} < V_B$, where the spectra are less populated (owing to low efficiency of HPGe detectors). Nordhagen *et al.* [32] and Stokstad *et al.* [33] have successfully demonstrated lifetime measurements in ^{59}Co, ^{63}Cu, ^{150}Nd, and ^{152}Sm using Doppler shape analysis of direct singles γ-ray spectra to be in good agreement with those from independent measurements.

The γ rays are emitted in-flight, with the recoiling ^{120}Sn nuclei in relative motion with respect to the detectors in the array and thus exhibit Doppler effect as expected. The heavy-^{32}S beam facilitates large excitation probability of the target and imparts substantial recoil velocity ($\beta \approx 2\%$) to the scattered nuclei. This is manifested into larger Doppler broadening of the emitted γ rays as shown in Fig. 1. Owing to inelastic scattering of ^{120}Sn recoils with a wide angular coverage as permitted by two-body kinematics (see inset of Fig. 1), each HPGe detector recorded an inclusive decay spectrum for scattering at all possible recoil directions. As ^{32}S is a spherical nucleus with well-defined excited states beyond 2 MeV, any contaminant γ energies in our region of interest arising from projectile excitation are avoided.

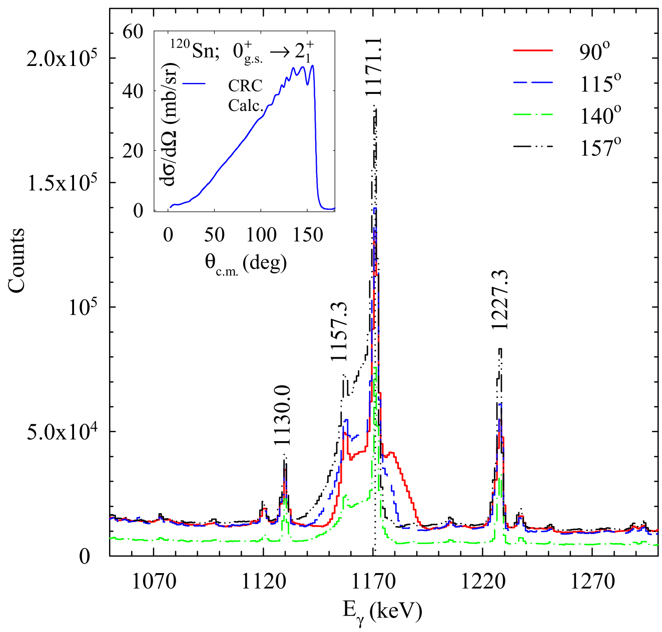

FIG. 1. Raw γ-ray spectra recorded in HPGe clovers at different angular positions in the laboratory frame for the ^{32}S + ^{120}Sn system. The most dominant transition corresponds to the decay of the 2_1^+ excited state of ^{120}Sn at 1171 keV. Inset shows the calculated angular distribution of the scattered ^{120}Sn nuclei in the center-of-mass frame (the moving source for the decay) at $E_{\rm lab} = 120$ MeV.

The origin of the additional peaks observed along with those from ^{120}Sn (Fig. 1) have been ascertained from the coincidence analysis of a symmetric E_γ-E_γ matrix. These peaks could be ascribed to the deexciting residues produced in the fusion-evaporation reaction of the ^{32}S beam with oxygen in the partially oxidized ^{120}Sn target. The dominant products of such a reaction include ^{39}K, ^{42}Ca, ^{43}Sc, etc., as indicated in statistical model calculations with the PACE [34] code as well as in experimental data on the decay of the same compound nucleus (^{48}Cr) at similar excitation energies [35]. The 1227-keV peak, for instance, is presumably from the decay of ^{42}Ca and ^{43}Sc nuclei while that at 1130 keV can be attributed to a long-lived state ($\tau \approx 12$ ps) in ^{39}K [36]. Most importantly, the 1157-keV peak, riding on the Doppler shape of the peak of interest (1171 keV), is from a long-lived ($\tau \approx 8.1$ ps) state in ^{43}Sc [37] and is not expected to affect the subsequent analysis or the results therefrom.

III. LIFETIME ANALYSIS

Lifetime analysis of the 2_1^+ state in ^{120}Sn has been carried out using the developments by Das *et al.* [38] in conjunction with the LINESHAPE [39] package. The analysis principally incorporates the trajectories of the scattered ^{120}Sn nuclei traversing in the target and the backing media wherein additional considerations consequent to the use of thick target are appropriately imbibed. The latter include evolving energy of the beam, and the consequent angular distribution of the scattering cross section, along the target depth as well as energy-angle distribution of the scattered nuclei respective

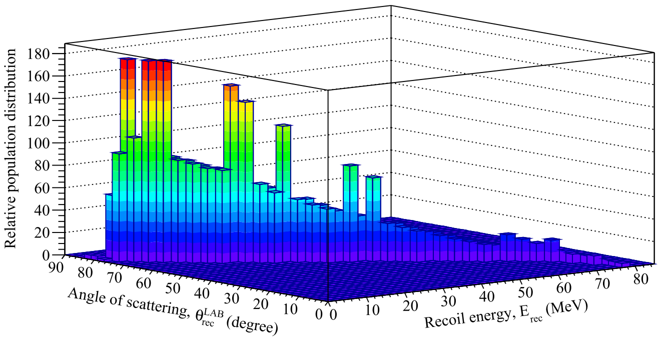

FIG. 2. Typical calculated relative population distribution of the scattered ^{120}Sn recoils in their 2_1^+ excited state as a function of laboratory scattering angle $\theta_{\rm rec}^{\rm LAB}$ and kinetic energy $E_{\rm rec}$ in the ^{32}S + ^{120}Sn system at $E_{\rm lab} = 120$ MeV.

to the changing beam energies. This determines the relative population distribution of the recoils (see Fig. 2). These trajectories are used to determine the velocity profiles of the scattered nuclei, as viewed by the γ-detectors and, with input of the level scheme information, to calculate the Doppler shape of the γ rays of interest. The implementation of this methodology in the present context is elaborated hereafter.

Given the substantial thickness of the target foil that leads to appreciable energy loss of the incident beam, the cross section for inelastic excitation of the ^{120}Sn nucleus to its 2_1^+ state at different beam energies along the target thickness has been estimated in the framework of a CRC model using FRESCO [40]. The calculations have been performed by coupling the major direct reaction channels to the entrance channel, such as (i) the low-lying 2_1^+ and 3_1^- states of ^{120}Sn at $E_x = 1.171$ MeV and 2.401 MeV, respectively, treated as collective vibrational one-phonon states with $B(E2; 0_{\rm g.s.}^+ \to 2_1^+) = 0.21\ e^2{\rm b}^2$ [25] and $B(E3; 0_{\rm g.s.}^+ \to 3_1^-) = 0.09\ e^2{\rm b}^3$ [4]; (ii) the first-excited 2^+ state of ^{32}S lying at 2.231 MeV, with $B(E2; 0_{\rm g.s.}^+ \to 2_1^+) = 0.033\ e^2{\rm b}^2$ and static quadrupole moment $Q_S(2_1^+) = -0.20$ b [41]; and (iii) transfer channels corresponding to pickup of neutron(s), (^{32}S, ^{33}S) and (^{32}S, ^{34}S), with unit spectroscopic factors. The coupling effects of excited states of ^{120}Sn with higher multipolarities or of multiphonon nature are found to be negligible. For instance, the excitation probability of the 4_1^+ state at $E_x = 2.194$ MeV, coupled as a double-quadrupole phonon state, is found to be very poor. The projectile-target interaction is governed by the Coulomb potential as well as an optical nuclear potential of Woods Saxon form, with a short-ranged imaginary part to account for the fusion process. The effect of nuclear coupling on the excitation of the 2_1^+ state in ^{120}Sn is found to be inconsequential, and the angular distribution of the scattering cross section is primarily governed by the Coulomb interaction. The calculations indicate a sharp decline in the $0_{\rm g.s.}^+ \to 2_1^+$ excitation cross section at beam energies below 95 MeV. Consequently, a target thickness of $\approx$3.2 mg/cm^2 can be ascribed to the production of the ^{120}Sn recoils in their 2_1^+ excited state and thus of the deexciting γ rays (effective production thickness). The remaining thickness of the target foil and the Au backing operate only as stopping media for the energetic recoils. The production thickness of the target was binned into six divisions of decreasing beam energy, each characterized by individual energy-angle distribution of the scattered ^{120}Sn nuclei in the 2_1^+ state.

One of the key inputs, as well as a significant source of uncertainty, in DSAM analysis is the simulation of trajectories of the recoiling nuclei of interest traversing in the target and the backing media. Strongly dependent on the stopping power of these media, the trajectories are typically represented by the velocity (β) and the direction (direction cosines) of the recoiling nuclei in uniform time steps. It is understood that the uncertainties on the stopping powers would affect the simulations and eventually the lifetime results. There have been several approaches for determining the stopping powers, principally through theoretical modeling based on available experimental data. One of the early developments in this domain was put forth by Blaugrund [42] based on the theory of electronic and atomic collisions of Lindhard *et al.* [43] to calculate specific energy losses of recoiling ions. The quoted uncertainty on the stopping powers estimated therefrom is within 20–25% [43]. This is of significance in the present context since the analysis of Sie *et al.* [28] that led to the lifetime result of the 2_1^+ state in ^{120}Sn to be $\tau_{2_1^+} \approx 1$ ps is entirely based on the Blaugrund formalism. Later developments in the stopping power modeling include those by Ziegler [44] as well as Northcliffe and Schilling [45]. These are essentially based on the proton and α stopping data applied to scaling algorithms for calculating the stopping powers for heavy ions. The results therefrom have been found to be discrepant, particularly at low kinetic energies [46]. These models have been adopted in the lineshape analyses of Refs. [22,23] as reported by Jungclaus *et al.*

A more rigorous approach incorporating Monte Carlo calculations in the treatment of nuclear scattering was demonstrated by Currie [47] to be superior to an analysis using Blaugrund's formalism. The corresponding γ-ray shapes were accompanied by lower uncertainties. However, the weakest point continued to be the uncertainties in absolute stopping powers. This can be remedied with the use of the contemporary SRIM + TRIM [44] packages, involving a database of updated and experimentally benchmarked stopping powers for heavy ions in a wide variety of media, with an uncertainty of a modest $\approx$5% [48] and known to be highly reliable in the kinetic energy range of 0.001–1000 MeV/nucleon [46]. The present analysis is based on the stopping powers calculated in the SRIM code and simulation of trajectories carried out using the TRIM program as implemented in the methodology developed by Das *et al.* [38]. The trajectories of the ^{120}Sn nuclei, through the target and backing foils, have been simulated in time steps of 0.002 ps. The origin of the trajectories were distributed across the production thickness of the target binned into six divisions as per the evolving excitation cross section of the ^{120}Sn in the 2_1^+ state.

The simulated trajectories were used to calculate the velocity profiles of the recoils, as viewed by the different detectors, using the HISTAVER program of the LINESHAPE package. The inputs therein, apart from the simulated trajectories, were target-detector distance, detector radius, and detector angles (θ, ϕ) with respect to the beam direction. The velocity profiles were calculated for individual (clover) detectors at different

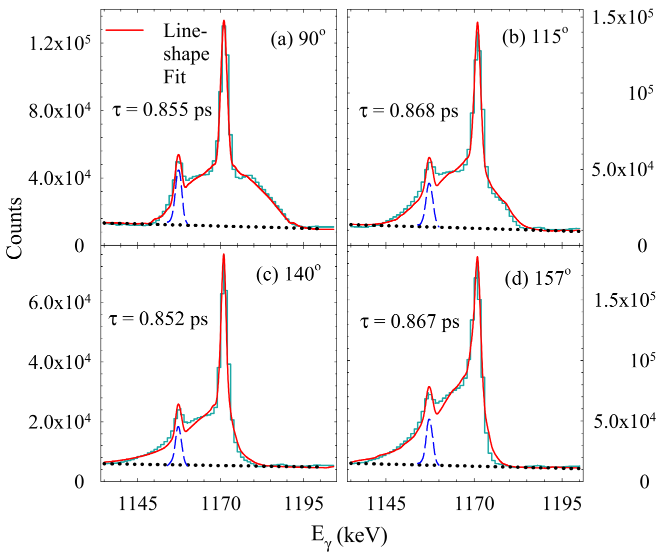

FIG. 3. Experimental Doppler broadened γ spectra and the results of the LINESHAPE calculations (solid lines) for the $2_1^+ \rightarrow 0_{\mathrm{g.s.}}^+$ decay in ^{120}Sn, at $E_x = 1171$ keV, are shown along with the linear fit of the background (dotted lines). The dashed lines represent deconvoluted fit of the additional stopped peak from the decay of a long lived ($\tau \approx 8.1$ ps) state in ^{43}Sc [37] and is not expected to affect the lineshape of the 1171-keV peak. The lifetime values in the individual figures follow the least-squares fitting of the experimental spectrum at the respective angle. The final value for the lifetime has been extracted from simultaneous fitting of the spectra at all angles (please see text).

angles, for analyzing individual detector spectra. The LINESHAPE code uses these velocity profiles and the level scheme inputs (transition energy, side feeding intensity, etc.) to calculate Doppler shapes of the γ ray of interest at different angles. The calculated shapes are least-squares fitted to the experimental spectra to extract the results of level lifetime, $\tau_{2_1^+}$, and transition quadrupole moment, Q_{02} [39].

The fitting parameters include the level lifetime, transition quadrupole moment, the side feeding (if any) time and spectral parameters such as the background and the height of any additional contaminant peak in the fitting range. In the current analysis, single detector (clover) spectra at 11 different (θ, ϕ) positions have been fitted simultaneously as per the standard procedure [49], which facilitates to constrain the multiple parameters associated with the minimization exercise. Figures 3(a)–3(d) illustrate typical fits of the γ-ray peak of interest, 1171 keV from ^{120}Sn, represented by continuous curves. The fitting exercise incorporated the 1157-keV peak riding on the Doppler shape of the 1171 keV. A lifetime value of $\tau_{2_1^+} = 0.863^{+0.029}_{-0.036}$ ps, and a transition quadrupole moment of $Q_{02} = 1.468^{-0.024}_{+0.033}$ eb, are obtained from this analysis. The quoted uncertainties were derived from χ^2 analysis of the fitted values and do not include the systematic effect of the uncertainties on the stopping powers. However, given that these were from the SRIM code, the uncertainties therefrom are known to be ≈5% [48] and significantly less than the earlier models used in conventional analyses.

Another uncertainty in lifetime analysis, following DSAM, pertains to (side) feeding from states above the level of interest. If these cannot be accounted appropriately, then the lifetime result on the state of interest is, at best, an upper limit of the same. As per the level scheme of ^{120}Sn [50], the 2_1^+ state is fed by $E2$ decays from (i) the 4_1^+ state via 1023-keV, (ii) the 0_2^+ state via 704-keV, and (iii) the 2_2^+ state via 926-keV transitions. These are, however, not expected to impact the aforementioned lifetime result of the 2_1^+ state due to the following factors. As per the CRC calculations, the population of these feeder states is rather low. These states are long lived ones [50] and feeding therefrom is expected to be insignificantly Doppler affected. The feedings were nevertheless incorporated into the analysis, with intensity ≈10% for the expectedly strongest $4_1^+ \rightarrow 2_1^+$ branch at the chosen bombarding energy, and observed to cause a variation in the lifetime result of the 2_1^+ level within the quoted uncertainties. The side feeding from the 3_1^- state ($E_x = 2401$ keV), through 1228-keV transition, has been found to be insignificant in this case. In fact, the statistics on the 1171-keV peak, with gate on 1228-keV transition in the angle-dependent matrices, is rather sparse for any conclusive analysis.

Traditionally, the analysis of the Doppler shapes or shifts are preferably carried out with coincident spectra corresponding to a gate set on a transition above the transition of interest in a cascade. Such an implementation eliminates the effects of any feeding, other than the gating one, and facilitates in improving the accuracy of the measurement. As far as the current measurement is concerned, the 1023-keV transition from the decay of the 4_1^+ state could have qualified for the purpose, and the lifetime analysis of the 2_1^+ level could have been pursued with gated spectra of the 1023-keV transition. However, as it has been brought out in the preceding text, the feeding from the 4_1^+ level is inconsequential and the corresponding coincidence spectra, with gate set on 1023-keV transition, are plagued with dearth of sufficient statistics for reliable fitting (not shown here). It is worth noting that the 4_1^+ level is long lived ($\tau_{4_1^+} \approx 2$ ps) [50] compared to the 2_1^+ state. Consequently, only a part of this feeding population contributes to the Doppler shape of the 1171-keV transition, deexciting the 2_1^+ state, further vexing the analysis in the top-gated spectra (contribution is primarily to the stopped component at 1171 keV). To verify this claim, the Doppler shape analysis could be pursued for the 1023-keV transition in the coincident spectra with gate on 1171 keV and lifetime of the 4_1^+ state be extracted therefrom. Figures 4(a)–4(c) illustrate the representative fits obtained from asymmetric angular matrices, with 90° detectors on one axis and one of the backward angles (157°, 140°, 115°) detectors on the other axis, with gate set on the 1171-keV transition at the 90° detectors. The corresponding lifetime, $\tau_{4_1^+} = 1.77^{+0.084}_{-0.089}$ ps, translates into a $B(E2; 4_1^+ \rightarrow 2_1^+) = 0.041^{+0.002}_{-0.003}$ e^2b^2, in compliance with the previously published [4] value of 0.035(11) e^2b^2. Since the lifetime analysis of the 4_1^+ state has been carried out with a gate set on a transition below the transition of interest, it may be argued that $\tau_{4_1^+}$ is actually an upper limit on the same. However, realistically speaking, the excitation reaction used herein has tenuously populated the states that

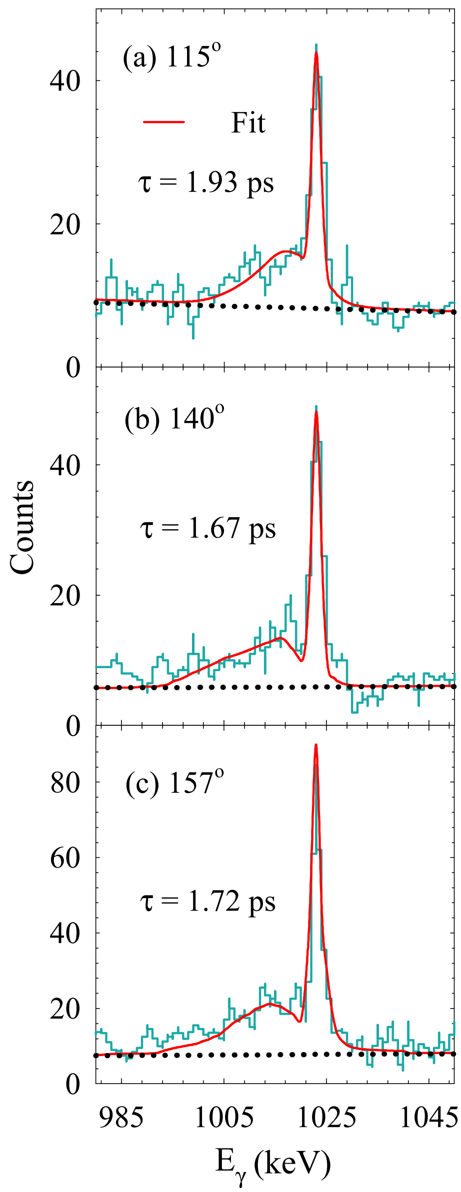

FIG. 4. γ-ray spectra gated with the $2_1^+ \rightarrow 0_{\mathrm{g.s.}}^+$ transition (1171 keV) in ^{120}Sn showing the coincident $4_1^+ \rightarrow 2_1^+$ transition (1023 keV). Asymmetric angular matrices, 90° versus (157°, 140°, 115°), have been used for generating the coincidence spectra with gate set on the 1171-keV transition at the 90° detectors. The fits to the accompanying weak structure of the $E2$ decay peak lead to the lifetime, $\tau_{4_1^+}$, of the decay. The lifetime values in the individual figures follow the least-squares fitting of the experimental spectrum at the respective angle. The final value for the lifetime has been extracted from simultaneous fitting of the spectra at all angles.

are still higher up in the excitation scheme of ^{120}Sn, following which the aforementioned value of $\tau_{4_1^+}$ can be perceived as its actual, at least within the purview of the present analysis. It may thus be concluded that the contributions from the dominant feeder levels to the broadened shape of the 1171-keV peak is insignificant and the result of $\tau_{2_1^+} = 0.863^{+0.029}_{-0.036}$ ps is equivalent to the mean lifetime of the 2_1^+ state.

TABLE I. Lifetime τ and transition probability $B(E2)$ for the $\lambda = 2$ (1171-keV) excitation in ^{120}Sn, compared with a few recent estimates.

$\tau_{2_1^+}$ (ps)	$B(E2; 0_{\mathrm{g.s.}}^+ \rightarrow 2_1^+)$ (e^2b^2)	Method	Ref.
$0.863^{+0.029}_{-0.036}$	$0.215^{-0.007}_{+0.009}$	DSAM	This work
—	0.215(9)	(^{7}Li, ^{7}Li′)	[9]
—	0.217(20)	(^{12}C, ^{12}C′)	[11]
0.97(5)	0.191(10)	DSAM	[22]
—	0.210(9)	CoulEx.	[25]
—	0.188(7)	CoulEx.	[24]

IV. RESULTS

From the measured lifetime $\tau_{2_1^+}$, the transition probability for the $2_1^+ \rightarrow 0_{\mathrm{g.s.}}^+$ decay with $E_\gamma^0 = 1.171$ MeV was deduced as follows:

$$\frac{1}{B(E2; 2_1^+ \rightarrow 0_{\mathrm{g.s.}}^+)} = 1.225 \times 10^9 \left(E_\gamma^0\right)^5 \tau_{2_1^+}. \qquad (1)$$

With $B(E2; 2_1^+ \rightarrow 0_{\mathrm{g.s.}}^+) = (\frac{1}{5})B(E2; 0_{\mathrm{g.s.}}^+ \rightarrow 2_1^+)$, the results of the lifetime and the transition probability are summarized in Table I, along with the estimates from a few recent measurements. It may be emphasized here that the results of $\tau_{2_1^+}$ and $B(E2; 0_{\mathrm{g.s.}}^+ \rightarrow 2_1^+)$ are not grossly different from the existing values. This affirms that the partial oxidation of the production thickness of the target foil may not have been veritable enough to significantly affect the stopping power (compared to that of elemental Sn), and a vast majority of the excited Sn recoils are slowed down in the enriched Sn medium. The consequent uncertainty, if any, is presumably covered within the statistical uncertainty of the lifetime result. As a case study, Ref. [49] reports a measurement on the level lifetimes in ^{32}P populated in a reaction involving an oxidized target. In the absence of absolute quantification of oxide phases in the target, a large deviation from the expected value is shown for the lifetime of the 1755-keV state in ^{32}P with variations in assumed density of the target foil. In comparison, the partial oxidation in the present work can be expected not to have affected the density of the target foil in the region where the slowing down occurs, thereby leading to a realistic lifetime numbers of worth and reason. Given the accuracy of the methodology adopted in the present work, with lower uncertainty on the stopping power, the present result is an improved estimate of the 2_1^+ level lifetime in ^{120}Sn by the DSAM method.

A. Enhanced $B(E2; 0_{\mathrm{g.s.}}^+ \rightarrow 2_1^+)$

The result from lifetime analysis confirms enhanced collectivity in the 2_1^+ excitation in ^{120}Sn, with $B(E2)/B(E2)_{\mathrm{sp}} \approx 12.3$, where $B(E2)_{\mathrm{sp}}$ gives the standard Weisskopf single-particle estimate [13]. The present result is compared with some recent estimates of $B(E2)$ for the Sn isotopes by different techniques, namely Coulomb excitation, lifetime measurement and heavy-ion scattering, in Fig. 5. The results deduced from the present and existing lifetime analyses do not include the systematic uncertainties from the stopping powers, which

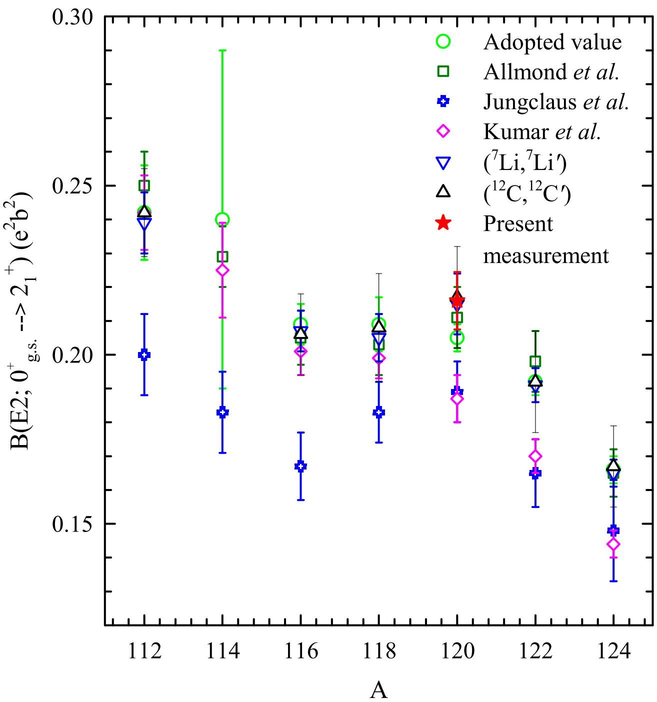

FIG. 5. Systematic plot of $B(E2; 0^+_{\text{g.s.}} \to 2_1^+)$ values for the stable even-mass Sn isotopes using the data obtained from existing measurements [9,11,12,22,24,25] and the one from the present measurement for the ^{120}Sn isotope.

are ≈5% and ≈10%, respectively. It is noteworthy that the present result is in very good agreement with the $B(E2)$ value reported by Allmond *et al.* [25] as well as with the recent results from heavy-ion-scattering measurements with ^{7}Li [9] and ^{12}C [11] projectiles. It has been suggested [1] that heavy-ion inelastic scattering preferentially excites nuclear states having a collective nature, thus supporting the result of the present work. While the results of Kumar *et al.* are in agreement with those of Allmond *et al.* for $^{112-118}$Sn, they are closer to the results of Jungclaus *et al.* for $^{120-124}$Sn, in contradiction to the result of this work.

B. Nonzero moment of inertia for the 2_1^+ state

In the course of this work, an attempt has been made to unambiguously determine the mean lifetime for the 2_1^+ state in ^{120}Sn. The corresponding Q_{02} value is also extracted. The comparison of experimental and theoretical values of structural parameters of excited states provides a test for the validity of nuclear models. A survey [51] of the spin-parity of first excited states in even-even nuclei shows that they are predominantly 2^+ and are often found to be of collective vibrational or rotational nature. The low-lying 2_1^+ states in rare-earth even-even nuclei with cylindrical symmetry in the body-fixed frame, depopulated by enhanced $E2$ ($2_1^+ \to 0^+_{\text{g.s.}}$) transitions and with large static quadrupole moments, were recognized by Bohr and Mottelson [52] as the missing levels of their ground-state rotational bands, with characteristic moments of inertia. While such ground-state bands are not found in spherical nuclei, theoretical estimates [53] as well as several measurements of nonzero static quadrupole moments for the 2_1^+ states in such nuclei are at variance with the near-harmonic vibrational model of excitations, which associates no rotational energy to degrees of freedom corresponding to a spherical symmetry. Although the accuracy of determination of static quadrupole moments in excited states is not appreciable (50–100%) as that for transition quadrupole moments (2–10%) [54], a conclusion can be drawn about the existence of a nonvanishing moment of inertia, $\mathcal{I}_{2_1^+} \neq 0$, in excited 2_1^+ states of spherical nuclei. For instance, the static electric quadrupole moment of 2_1^+ state of ^{120}Sn has previously been determined by means of the reorientation effect [2,3] and is found to be small, 0.09 ± 0.10 eb but nonzero. The characteristics of both the ground-state deformed and ground-state spherical nuclei have been successfully unified with the idea of spin-dependent moment of inertia for a wide range of even-even nuclei by means of the semiclassical variable moment of inertia (VMI) model [55] that defines an energy spectrum of states exhibiting rotational character,

$$E_J(\mathcal{I}_J) = \frac{1}{2}C\left(\mathcal{I}_J^2 - \mathcal{I}_0^2\right) + \frac{1}{2\mathcal{I}_J}J(J+1). \tag{2}$$

The parameters C and $\mathcal{I}_0$ are the restoring force constant and the ground-state moment of inertia, respectively. The equilibrium condition $\partial E_J(\mathcal{I}_J)/\partial \mathcal{I}_J = 0$ determines $\mathcal{I}_J$ as the moment of inertia (in units of $\hbar^2$) for a state J. For a ground-state spherical nucleus, the above prescription can be written in the limit of $\mathcal{I}_0 \to 0$ as

$$E_J(\mathcal{I}_J) = \frac{3}{4}\frac{J(J+1)}{\mathcal{I}_J}. \tag{3}$$

The VMI model proposes an empirical relationship [55,56] between the $2_1^+ \to 0^+_{\text{g.s.}}$ transition quadrupole moment, Q_{02}, and transition moment of inertia, $\mathcal{I}_{02}$, for nuclei in the mass range $12 \leqslant A \leqslant 252$ as:

$$Q_{02} = KA^{1/4}\sqrt{\mathcal{I}_{02}}, \tag{4}$$

where $K = 10.5$ eb keV$^{1/2}$ and $\mathcal{I}_{02}^2 = \frac{1}{2}(\mathcal{I}^2_{0^+_{\text{g.s.}}} + \mathcal{I}^2_{2_1^+})$ [56]. The correlation between values of transition quadrupole moments from Ref. [57] and moments of inertia given by the VMI model [55] is shown in Fig. 6 for several even-even nuclei (hollow symbols) with atleast some states of rotational character. The curve represents the best-fit to Eq. (4).

With the 2_1^+ state at $E_{2_1^+} = 1171$ keV in ^{120}Sn, a value of $\mathcal{I}_{2_1^+} \approx 0.00384$ keV^{-1} is obtained. The Q_{02} value from Table I is plotted against the VMI model-predicted $\mathcal{I}_{02}$, as shown by the filled symbol in Fig. 6. The symbol falls on the best-fit curve. This confirms presence of anharmonicity in the $0^+_{\text{g.s.}} \to 2_1^+$ intrinsic excitation is ^{120}Sn, suitably explained by the existence of a nonvanishing angular momentum dependent moment of inertia. Measurements of level lifetimes and transition quadrupole moments can thus be an important tool to test nuclear models.

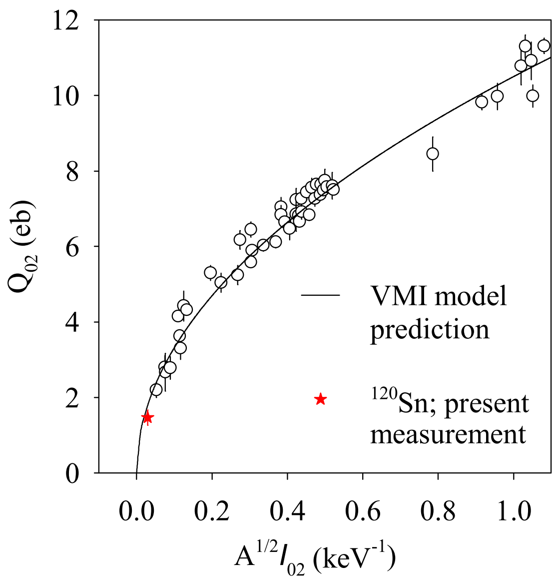

FIG. 6. Transition quadrupole moment Q_{02} versus $A^{1/2}\mathcal{I}_{02}$ for a wide range of nuclei. The abscissae have been calculated by the VMI model in Ref. [55]. The data for Q_{02} (hollow circles) are taken from Ref. [57]. The solid curve gives the best-fit to Eq. (4). The red solid symbol represents the result of the present work, with Q_{02} extracted from DSAM lifetime analysis and $\mathcal{I}_{02}$ calculated using VMI model prescription.

V. SUMMARY

The mean lifetime of the 2_1^+ level in ^{120}Sn ($E_x = 1171$ keV) has been determined using DSAM implemented through updated methodologies, and the corresponding $B(E2; 0^+_{\mathrm{g.s.}} \rightarrow 2_1^+)$ value is deduced therefrom, signaling enhanced collectivity. Independent measurements of 2_1^+ lifetime over the years have reported discrepant transition probabilities and collective properties. The present result is in excellent agreement with the results of Allmond *et al.*, where the $B(E2)$ value has been measured in conjunction with the static electric quadrupole and magnetic dipole moments. Several theoretical estimates focused on reproducing the existing $B(E2)$ results for the unstable neutron-rich and the neutron-deficient Sn isotopes predict much lower $B(E2)$ values for the stable Sn isotopes. This spells out the need for improved theoretical calculations for the $^{100-136}$Sn chain. The present result is an improved estimate of the 2_1^+ level lifetime in ^{120}Sn, characterized by lower uncertainties compared to previous efforts. An estimate of the 4_1^+ level lifetime is also presented, in compliance with the predicted value. A similar analysis for the other stable Sn nuclei may be expected to lead to a similar conclusion about enhancement of collectivity. The corresponding transition quadrupole moments can be useful as a test for arharmonicity in the 2_1^+ transition in the spherical Sn nuclei. A precise measurement of level lifetime also reduces uncertainty in the estimation of the proton transition matrix element [58], which, in conjunction with the neutron transition matrix element obtained from light- or heavy-ion-scattering experiments, would allow the determination of proton and neutron effective charges to be used in shell-model calculations of transition rates.

ACKNOWLEDGMENTS

The financial support of BRNS through Project No. 2012/21/11-BRNS/1090 is greatly acknowledged. We thank Dr. S. Mukhopadhyay, BARC, for several fruitful discussions. This work has been partially funded by the Department of Science and Technology, Government of India (Grant No. IR/S2/PF-03/2003-II). Technical help provided by S. Jadhav, B. S. Naidu, R. Donthi, and Abraham T. Vazhappilly during the preparation of the experiment is also acknowledged.

[1] W. T. Pinkston and G. R. Satchler, Nucl. Phys. **27**, 270 (1961).
[2] P. H. Stelson, F. K. McGowan, R. L. Robinson, and W. T. Milner, Phys. Rev. C **2**, 2015 (1970).
[3] R. Graetzer, S. M. Cohick, and J. X. Saladin, Phys. Rev. C **12**, 1462 (1975).
[4] N. G. Jonsson, A. Backlin, J. Kantele, R. Julin, M. Luontarna, and A. Passoja, Nucl. Phys. A **371**, 333 (1981).
[5] J. Bryssinck, L. Govor, V. Y. Ponomarev, F. Bauwens, O. Beck, D. Belic, P. von Brentano, D. DeFrenne, T. Eckert, C. Fransen *et al.*, Phys. Rev. C **61**, 024309 (2000).
[6] T. H. Curtis, R. A. Eisenstein, D. W. Madsen, and C. K. Bockelman, Phys. Rev. **184**, 1162 (1969).
[7] O. Beer, A. E. Behay, P. Lopato, Y. Terrien, G. Vallois, and K. K. Seth, Nucl. Phys. A **147**, 326 (1970).
[8] G. Bruge, J. C. Faivre, H. Faraggi, and A. Bussiere, Nucl. Phys. A **146**, 597 (1970).
[9] A. Kundu, S. Santra, A. Pal, D. Chattopadhyay, R. Tripathi, B. J. Roy, T. N. Nag, B. K. Nayak, A. Saxena, and S. Kailas, Phys. Rev. C **99**, 034609 (2019).
[10] L. R. Gasques, A. S. Freitas, L. C. Chamon, J. R. B. Oliveira, N. H. Medina, V. Scarduelli, E. S. Rossi, M. A. G. Alvarez, V. A. B. Zagatto, J. Lubian *et al.*, Phys. Rev. C **97**, 034629 (2018).
[11] A. Kundu, S. Santra, A. Pal, D. Chattopadhyay, T. N. Nag, R. Gandhi, P. C. Rout, B. J. Roy, B. K. Nayak, and S. Kailas, Phys. Rev. C **100**, 024614 (2019).
[12] S. Raman, C. Nestor, and P. Tikkanen, At. Data Nucl. Data Tables **78**, 1 (2001).
[13] J. M. Blatt and V. F. Weisskopf, *Theoretical Nuclear Physics* (Wiley & Sons Inc., New York, 1952).
[14] I. O. Morales, P. V. Isacker, and I. Talmi, Phys. Lett. B **703**, 606 (2011).
[15] A. Banu, J. Gerl, C. Fahlander, M. Górska, H. Grawe, T. R. Saito, H.-J. Wollersheim, E. Caurier, T. Engeland, A. Gniady *et al.*, Phys. Rev. C **72**, 061305(R) (2005).
[16] D. Radford, C. Baktash, J. Beene, B. Fuentes, A. Galindo-Uribarri, J. G. del Campo, C. Gross, M. Halbert, Y. Larochelle, T. Lewis *et al.*, Nucl. Phys. A **746**, 83c (2004).
[17] P. Doornenbal, P. Reiter, H. Grawe, H. J. Wollersheim, P. Bednarczyk, L. Caceres, J. Cederkäll, A. Ekström, J. Gerl, M. Górska *et al.*, Phys. Rev. C **78**, 031303(R) (2008).

[18] C. Vaman, C. Andreoiu, D. Bazin, A. Becerril, B. A. Brown, C. M. Campbell, A. Chester, J. M. Cook, D. C. Dinca, A. Gade *et al.*, Phys. Rev. Lett. **99**, 162501 (2007).

[19] P. Doornenbal, S. Takeuchi, N. Aoi, M. Matsushita, A. Obertelli, D. Steppenbeck, H. Wang, L. Audirac, H. Baba, P. Bednarczyk *et al.*, Phys. Rev. C **90**, 061302(R) (2014).

[20] A. Ansari, Phys. Lett. B **623**, 37 (2005).

[21] D. Rosiak, M. Seidlitz, P. Reiter, H. Naïdja, Y. Tsunoda, T. Togashi, F. Nowacki, T. Otsuka, G. Colò, K. Arnswald *et al.*, Phys. Rev. Lett. **121**, 252501 (2018).

[22] A. Jungclaus, J. Walker, J. Leske, K.-H. Speidel, A. Stuchbery, M. East, P. Boutachkov, J. Cederkäll, P. Doornenbal, J. Egido *et al.*, Phys. Lett. B **695**, 110 (2011).

[23] M. East, A. Stuchbery, A. Wilson, P. Davidson, T. Kibédi, and A. Levon, Phys. Lett. B **665**, 147 (2008).

[24] R. Kumar, M. Saxena, P. Doornenbal, A. Jhingan, A. Banerjee, R. K. Bhowmik, S. Dutt, R. Garg, C. Joshi, V. Mishra *et al.*, Phys. Rev. C **96**, 054318 (2017).

[25] J. M. Allmond, A. E. Stuchbery, A. Galindo-Uribarri, E. Padilla-Rodal, D. C. Radford, J. C. Batchelder, C. R. Bingham, M. E. Howard, J. F. Liang, B. Manning *et al.*, Phys. Rev. C **92**, 041303(R) (2015).

[26] B. Pritychenko, M. Birch, B. Singh, and M. Horoi, At. Data Nucl. Data Tables **107**, 1 (2016).

[27] H. Jiang, Y. Lei, G. J. Fu, Y. M. Zhao, and A. Arima, Phys. Rev. C **86**, 054304 (2012).

[28] S. Sie, J. Geiger, D. Ward, and H. Andrews, Rep. No. AECL-4147, Atomic energy of Canada Limited Progress Report, Ontario (1972), p. 14.

[29] B. Hrastnik, V. Knapp, and M. Vlatkovic, Nucl. Phys. **89**, 412 (1966).

[30] R. Palit, S. Saha, J. Sethi, T. Trivedi, B. S. Naidu, P. B. Chavan, R. Donthi, and S. Jadhav, J. Phys.: Conf. Ser. **420**, 012159 (2013).

[31] R. Palit, S. Saha, J. Sethi, T. Trivedi, S. Sharma, B. Naidu, S. Jadhav, R. Donthi, P. Chavan, H. Tan *et al.*, Nucl. Instrum. Methods A **680**, 90 (2012).

[32] R. Nordhagen, B. Elbek, and B. Herskind, Nucl. Phys. A **104**, 353 (1967).

[33] R. Stokstad, I. Fraser, J. Greenberg, S. Sie, and D. A. Bromley, Nucl. Phys. A **156**, 145 (1970).

[34] A. Gavron, Phys. Rev. C **21**, 230 (1980).

[35] C. M. Jachcinski, D. G. Kovar, R. R. Betts, C. N. Davids, D. F. Geesaman, C. Olmer, M. Paul, S. J. Sanders, and J. L. Yntema, Phys. Rev. C **24**, 2070 (1981).

[36] J. Chen, Nucl. Data Sheets **149**, 1 (2018).

[37] G. Ball, J. Forster, F. Ingebretsen, and C. Monahan, Nucl. Phys. A **180**, 517 (1972).

[38] S. Das, S. Samanta, R. Bhattacharjee, R. Raut, S. Ghugre, A. Sinha, U. Garg, R. Chakrabarti, S. Mukhopadhyay, A. Dhal *et al.*, Nucl. Instrum. Methods A **841**, 17 (2017).

[39] J. C. Wells and N. R. Johnson, Tech. Report ORNL-6689, Oak Ridge National Laboratory Physics Division, Oak Ridge (1991), p. 44.

[40] I. J. Thompson and F. M. Nunes, *Nuclear Reactions for Astrophysics* (Cambridge University Press, New York, 2009).

[41] K. Nakai, J. L. Québert, F. S. Stephens, and R. M. Diamond, Phys. Rev. Lett. **24**, 903 (1970).

[42] A. Blaugrund, Nucl. Phys. **88**, 501 (1966).

[43] J. Lindhard, M. Scharff, and H. E. Schiott, Mat. Fys. Medd. Dan. Vid. Selsk. **33** (1963).

[44] J. Ziegler, *The Stopping and Ranges of Ions in Matter* (Pergamon Press, London, 1980), Vol. 3.

[45] L. Northcliffe and R. Schilling, At. Data Nucl. Data Tables **7**, 233 (1970).

[46] H. Paul and A. Schinner, Nucl. Instrum. Methods B **209**, 252 (2003).

[47] W. Currie, Nucl. Instr. Methods **73**, 173 (1969).

[48] www.srim.org.

[49] R. Bhattacharjee, S. S. Bhattacharjee, K. Basu, P. V. Rajesh, R. Raut, S. S. Ghugre, D. Das, A. K. Sinha, L. Chaturvedi, U. Garg *et al.*, Phys. Rev. C **90**, 044319 (2014).

[50] K. Kitao, Y. Tendow, and A. Hashizume, Nucl. Data Sheets **96**, 241 (2002).

[51] G. Scharff-Goldhaber, Phys. Rev. **90**, 587 (1953).

[52] A. Bohr and B. R. Mottelson, Phys. Rev. **89**, 316 (1953).

[53] G. Watanuki, Y. Miyanishi, and M. Yasuno, Prog. Theor. Phys. **59**, 790 (1978).

[54] G. Scharff-Goldhaber, C. B. Dover, and A. L. Goodman, Annu. Rev. Nucl. Sci. **26**, 239 (1976).

[55] M. A. J. Mariscotti, G. Scharff-Goldhaber, and B. Buck, Phys. Rev. **178**, 1864 (1969).

[56] Y. P. Varshni and S. Bose, Phys. Rev. C **3**, 958 (1971).

[57] P. Stelson and L. Grodzins, Nucl. Data Sheets A **1**, 21 (1965).

[58] A. M. Bernstein, V. R. Brown, and V. A. Madsen, Comments Nucl. Part. Phys. **11**, 203 (1983).